

## Original Article

# A manzamine-derived compound as a potential therapeutic agent for glioma by inducing apoptosis and cell cycle arrest

Ya-Jui Lin<sup>1,2</sup>, Chiung-Yin Huang<sup>3</sup>, Ya-Ching Shen<sup>4</sup>, Kuo-Chen Wei<sup>1,3,5</sup>, Chi-Cheng Chuang<sup>1</sup>, Peng-Wei Hsu<sup>1</sup>, Yin-Cheng Huang<sup>1</sup>, Tsong-Long Hwang<sup>2,6,7,8,9</sup>, Pin-Yuan Chen<sup>5,10</sup>

<sup>1</sup>Department of Neurosurgery, Chang Gung Memorial Hospital, Linkou, Taiwan; <sup>2</sup>Division of Natural Product, Graduate Institute of Biomedical Sciences, Chang Gung University, Taoyuan, Taiwan; <sup>3</sup>Department of Neurosurgery, New Taipei Municipal Tucheng Hospital, Chang Gung Medical Foundation, New Taipei, Taiwan; <sup>4</sup>School of Pharmacy, College of Medicine, National Taiwan University, Taipei, Taiwan; <sup>5</sup>School of Medicine, Chang Gung University, Taoyuan, Taiwan; <sup>6</sup>School of Traditional Chinese Medicine, Chang Gung University, Taoyuan, Taiwan; <sup>7</sup>Research Center for Chinese Herbal Medicine, Research Center for Food and Cosmetic Safety, Graduate Institute of Health Industry Technology, Chang Gung University of Science and Technology, Taoyuan, Taiwan; <sup>8</sup>Department of Anesthesiology, Chang Gung Memorial Hospital, Taoyuan, Taiwan; <sup>9</sup>Department of Chemical Engineering, Ming Chi University of Technology, New Taipei City, Taiwan; <sup>10</sup>Department of Neurosurgery, Chang Gung Memorial Hospital, Keelung, Taiwan

Received December 7, 2021; Accepted March 31, 2022; Epub April 15, 2022; Published April 30, 2022

**Abstract:** Glioma is a severe disease with a poor prognosis despite aggressive surgical resection and traditional chemotherapies. Therefore, new anti-neoplastic drugs are urgently needed. Bioactive compounds from natural products are potential sources of antiproliferative molecules, among which manzamine compounds extracted from the Formosan marine sponge *Haliclona* sp. have shown considerable promise as anticancer drugs. In the present study, the anti-neoplastic effect and mechanism of the manzamine derivative 1-(9'-propyl-3'-carbazole)-1, 2, 3, 4-tetrahydro- $\beta$ -carboline (PCTC) were investigated using in vitro cell lines and an in vivo subcutaneous animal model. Both cytotoxic and anti-proliferative effects were shown in human and murine glioma cell lines (A172, U87MG, and GL261), together with enhanced expressions of apoptotic enzymes and intracellular reactive oxygen species, and blockage of the G1/S phase of the cell cycle. In addition, combined treatment of GL261 cells with PCTC and temozolomide had a synergic antiproliferative effect. Significant safety, efficacy, and survival benefits were also demonstrated with PCTC treatment in the murine subcutaneous GL261 model. In conclusion, PCTC could effectively promote cell death through apoptosis and cell cycle arrest in glioma cell lines, and provide survival benefits in the animal model. Therefore, PCTC may be a clinically beneficial therapy for glioblastoma.

**Keywords:** Glioma, natural product, apoptosis, cell cycle arrest

## Introduction

Glioma, and in particular glioblastoma multiforme (GBM), is the most common and aggressive primary malignant brain tumor, with a median overall survival of less than 15 months even after maximal surgical resection of the tumor followed by the Stupp protocol with radiotherapy plus concomitant and adjuvant chemotherapy (temozolomide; TMZ) [1]. Because of the aggressive and diffusely infiltrative nature, tumor recurrence is inevitable. It

often leads to rapid tumor spread to other brain regions and early local or marginal recurrence despite surgical resection [2, 3]. Although chemotherapy plays an important role in treating unresectable and recurrent tumors, there are currently no effective drugs for glioma. There are two major issues. First, the specialized blood-brain barrier (BBB) prevents most large molecules from penetrating into tumors. Second, drug resistance often occurs due to the molecular and cellular heterogeneity of glioma [4]. Therefore, developing new chemotherapeu-

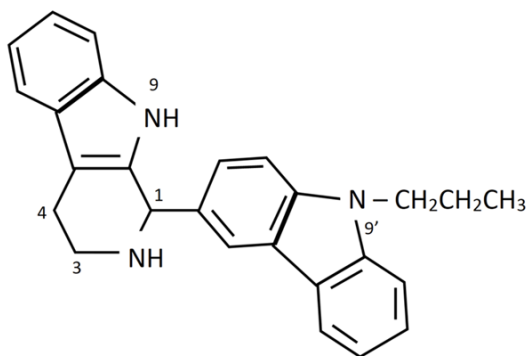


**Figure 1.** Chemical structure of 1-(9'-propyl-3'-carbazole)-1, 2, 3, 4-tetrahydro-β-carboline (PCTC).

tic agents to treat not only unresectable tumors but also infiltrating tumor cells may significantly improve treatment outcomes.

The natural world is a major source of small molecules that could be developed into novel pharmaceuticals, and compounds derived from natural products are considered to be potential sources of new anti-cancer drugs [5]. Manzamines are small molecules, and several have been isolated from the Formosan marine sponge, *Haliclona* sp. [6].

Manzamines isolated from sponges and other marine microorganisms are members of the β-carboline alkaloid family [7, 8]. Previous studies have shown that some manzamine derivatives have cytotoxic effects against human cancer cells [9]. Twelve manzamine-derived compounds have recently been synthesized, and their cytotoxic effects have been examined in four cancer cell lines from the lung (A549, H1299), liver (HepG2), and breast (MCF7). Of these 12 compounds, 1-(9'-propyl-3'-carbazole)-1, 2, 3, 4-tetrahydro-β-carboline (PCTC) (**Figure 1**) has shown the best cytotoxic activity [4]. In addition, the molecular weight of PCTC is around 379. It is difficult for molecules >400 Da to penetrate BBB [10]. PCTC is a potential chemotherapeutic drug to treat glioma. Therefore, the aim of this study was to investigate the anti-neoplastic effect of PCTC on glioma. We used an in vitro model and identified both cytotoxic and anti-proliferative effects of PCTC against glioma cells (A172, U87MG, and GL261 cell lines). We also tested the safety and efficacy in vivo in a GL261 subcutaneous implantation mice model.

## Materials and methods

### Ethics statement

All mouse experiments were conducted in accordance with the Guide for the Care and Use of Laboratory Animals published by the Institutional of Laboratory Animal Resources, National Research Council, U.S.A. The study protocol was approved by the Institutional Animal Care and Use Committee (IACUC) of Chang Gung Memorial Hospital in Taiwan. All experiments were following the ARRIVE guidelines. Surgical and experimental procedures were performed after the animals had been anesthetized with isoflurane inhalation (evaporation rate: 1-2%, flow rate: 800 ml/min), and all efforts were made to minimize animal suffering.

### Cells and cell culture

The human malignant glioma cell lines A172 and U87MG, and murine glioma cell line GL261 were purchased from the American Type Culture Collection. The glioma cells were cultured in Dulbecco's Modified Eagle Medium (DMEM; Thermo Scientific) supplemented with 10% heat-incubated fetal bovine serum (FBS; Thermo Scientific) and 1% Antibiotic-Antimycotic (Thermo Scientific), in an incubator with 5% CO<sub>2</sub> and 100% humidity at 37°C. Cells in the exponential phase of growth were used in all of the experiments.

### Cytotoxicity assay

Cytotoxicity (cell growth inhibition) induced by PCTC was analyzed using a Cell Counting Kit-8 colorimetric assay (CCK-8, Sigma-Aldrich). Briefly, the A172, U87MG and GL261 glioma cells were seeded into a 96-well plate, with each well containing 100 μl of cell suspension and approximately 5×10<sup>3</sup> cells. After incubation for 24 hours, the cells were washed with serum-free medium and then added to serum-free medium containing PCTC. An appropriate amount of CCK-8 solution (10 μl) was added to the culture medium, followed by incubation at 37°C for 60 minutes for the A127 and U87MG cells, and 120 minutes for the GL261 cells. Absorbance was measured at 450 nm using a microplate reader (Multiskan™ GO; Thermo Scientific) in accordance with the manufacturer's instructions.

For cell viability after PCTC and TMZ treatment, GL261 glioma cells were seeded into a 24-well plate ( $3 \times 10^4$  cells/well). After incubation with PCTC alone, TMZ alone, and a combination of PCTC and TMZ in 10% FBS for 24 hours, the treated cells were incubated with WST-1 assay reagent (Roche) for 2 hours. Absorbance was measured at 450 nm with 200  $\mu$ l medium.

### *Cell morphology and colony formation*

A172, U87MG, GL261 cells were seeded into a 6-well plate at  $1.5 \times 10^5$  cells/well. After incubation for 24 hours, the cells were washed with serum-free medium and then treated with PCTC. After incubation, cell morphology was observed under a phase-contrast microscope (IX81; Olympus). To assess colony formation, GL261 cells were seeded into a 6-well plate at  $1.5 \times 10^5$  cells/well. After incubation for 24 hours, the cells were added to culture medium containing PCTC. After 9 days, the medium was depleted. The cells were washed with iced phosphate buffered saline (PBS) twice, and then fixed in iced 4% paraformaldehyde for 10 minutes. After the supernatant was depleted, the cells were colored by crystal violet for 15 minutes. The cells were then washed with ddH<sub>2</sub>O until clean.

### *Flow cytometric analysis*

Glioma cells were seeded into a 6-cm dish at  $3 \times 10^5/\mu$ l. The dish was incubated at 37°C in a 5% CO<sub>2</sub> atmosphere for 24 hours. After washing with serum-free medium, the cells were incubated with serum-free medium containing PCTC or DMSO for 6 hours, and the number of cells was counted. The cells were suspended ( $10^6/\text{ml}$ ) in annexin V-binding buffer, and 100  $\mu$ l solution was colored using 5  $\mu$ l annexin V and 5  $\mu$ l povidone iodine (PI) away from light. The percentage of apoptotic cells was then analyzed using a flow cytometer (BD Accuri™ C6 Plus) and BD Accuri C6 software with an FITC Annexin V Apoptosis Detection Kit I (BD Biosciences) according to the manufacturer's instructions.

Glioma cells were seeded into a 96-well plate at  $5 \times 10^3/100$   $\mu$ l. The wells were incubated at 37°C in a 5% CO<sub>2</sub> atmosphere for 24 hours. After washing with serum-free medium, the cells were incubated with serum-free medium containing PCTC. After returning to room temperature, 100  $\mu$ l Caspase-Glo® 3/7 Assay so-

lution was added to each well, and then stirred at 400 rpm for 30 seconds. After 1 hour at room temperature and away from light, the luminance was measured.

### *Measurement of intracellular reactive oxygen species*

A172, U87MG, GL261 glioma cells were seeded into 4 wells of a 48-well plate. Each well contained 500  $\mu$ l of cell suspension at approximately  $10^5$  cells/ml. The plate was incubated at 37°C in a 5% CO<sub>2</sub> atmosphere for 24 hours. After washing with serum-free medium, the cells were incubated with serum medium containing PCTC with or without N-acetyl-L-cysteine (NAC, Sigma). The supernatant was then depleted, and the remaining cells were incubated with 400 mM 2',7'-dichlorofluorescein diacetate (DCFDA; Santa Cruz Biotechnology) for 30 minutes. Fluorescence intensity was measured using a fluorescence microscope (IX81; Olympus) equipped with laser-induced fluorescence (Lumen 200 fluorescence Illumination System, Prior Scientific). Flow cytometry was also performed.

### *Western blotting*

GL261 cells were treated with PCTC for the indicated periods. Samples were washed with PBS and lysed for 30 min on ice using RIPA lysis buffer (Thermo, USA). Protein samples were prepared by SDS-PAGE and transferred to PVDF membranes. The membranes were blocked and probed with primary antibodies overnight at 4°C against Bcl2, PARP, p38, JNK. After extensive washing and incubation with secondary antibodies, the blots were visualized using Amersham Hyperfilm ECL (GE Healthcare).

### *Measurement of cell cycle arrest*

GL261 cells were seeded onto a 6-cm culture dish ( $3 \times 10^5$  cells) overnight, and then treated with DMSO and PCTC 4  $\mu$ M in serum-free medium for 24 hours. The cells were trypsinized and centrifuged for 5 minutes at 200 g. After the supernatant had been decanted, the cells were fixed in 70% ethanol at 4°C. Finally, the cells were incubated with 1 ml PI solution mix (50  $\mu$ g/ml PI + 0.1 ml/ml RNase + 0.05% TritonX-100) for 30 minutes without bright light at 37°C. The cellular DNA content of the treated cells was analyzed by flow cytometry (BD Accuri™ C6 Plus).

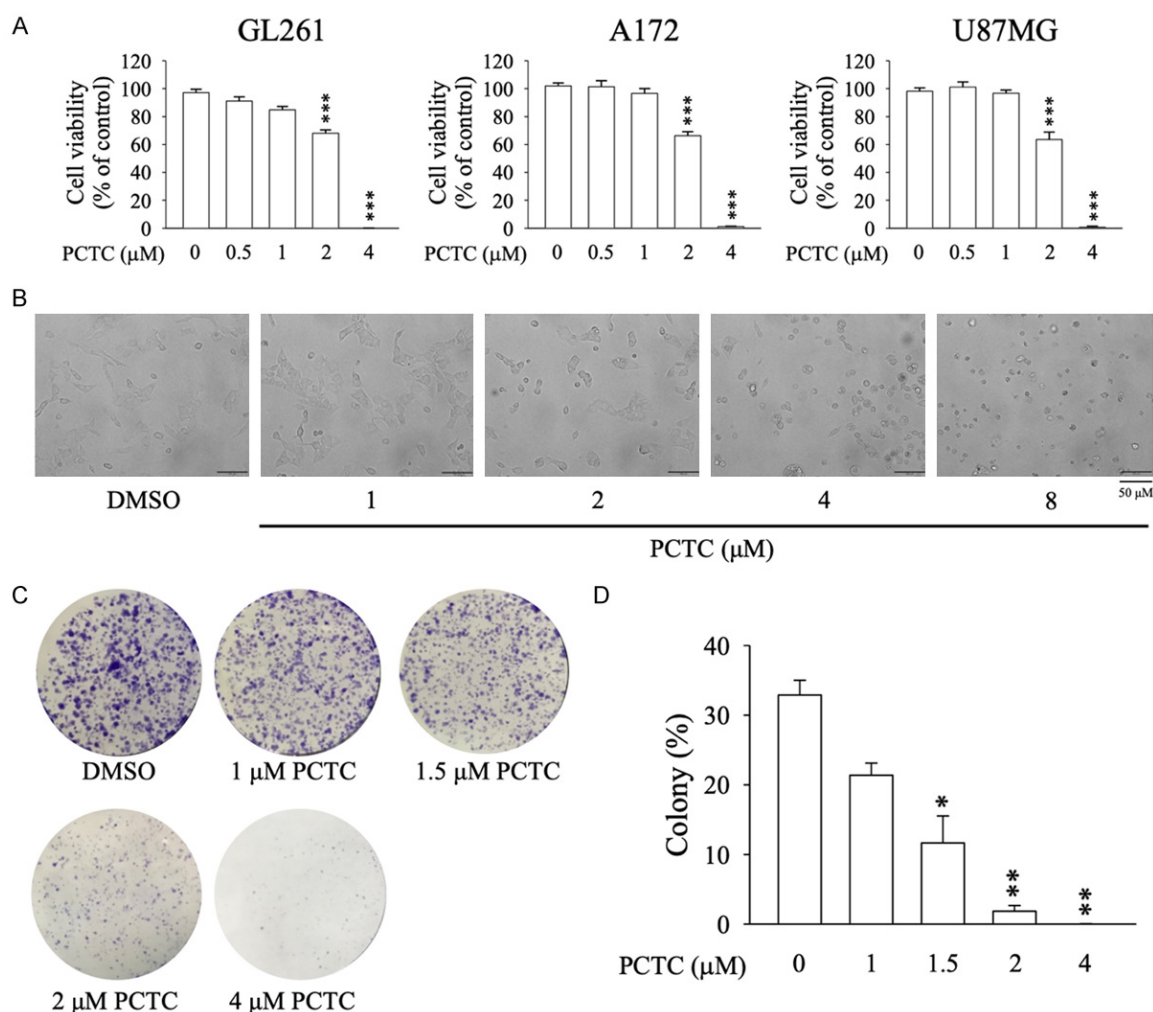


**Figure 2.** The manzamine-A derivative PCTC induced in vitro cytotoxicity in glioma cell lines. A. PCTC induced dose-dependent cytotoxicity in glioma A172, U87MG and GL261 cell lines after 24 hours, N=3 biological replicates. B. Microscopic analysis showed apoptotic-like morphological destruction after different doses of PCTC treatment for 24 hours in the GL261 glioma cells. C. Reduced colony formation of GL261 cells on Day 9. D. Bar graph showing measurements of the areas of colony formation of GL261 cells after PCTC treatment. \* $P < 0.05$ ; \*\* $P < 0.01$ ; \*\*\* $P < 0.001$ , t-test.

#### *In vivo tumor model*

Six- to eight-week-old C57BL/6 mice were obtained from Bio Lasco Taiwan, Inc. During the experimental period, the mice were kept in a cage and housed in a temperature- and humidity-controlled aseptic room provided with a light/dark cycle system. GL261 glioma cells ( $5 \times 10^5$ ) were suspended in 50  $\mu\text{L}$  of DMEM and subcutaneously injected into the right flank of the mice (weight  $20 \pm 2$  g [mean  $\pm$  SD]). Before tumor implantation, the animals were anesthetized with isoflurane inhalation (evaporation rate: 1-2%, flow rate: 800 ml/min). The mice were then untreated (control), treated with DMSO (sham), or treated with PCTC (10 mM/25  $\mu\text{L}$ ) via tail vein injection on Day 11, 14, and 18.

Tumor size was measured directly using a ruler. The survival of each group was also assessed.

#### **Results**

##### *Cytotoxicity to glioma*

We examined the anticancer effects of PCTC in three glioma cell lines (A172, U87MG, GL261). Dose-dependent cytotoxicity was identified using a CCK-8 assay after treatment with PCTC for 24 hours (**Figure 2A**). A significant dose-dependent inhibitory effect was noted in all three glioma cell lines with a concentration  $\geq 2$   $\mu\text{M}$ . Microscopic analysis of three glioma cells at 24 hours after PCTC treatment revealed gradual inhibition of the growth of the glioma



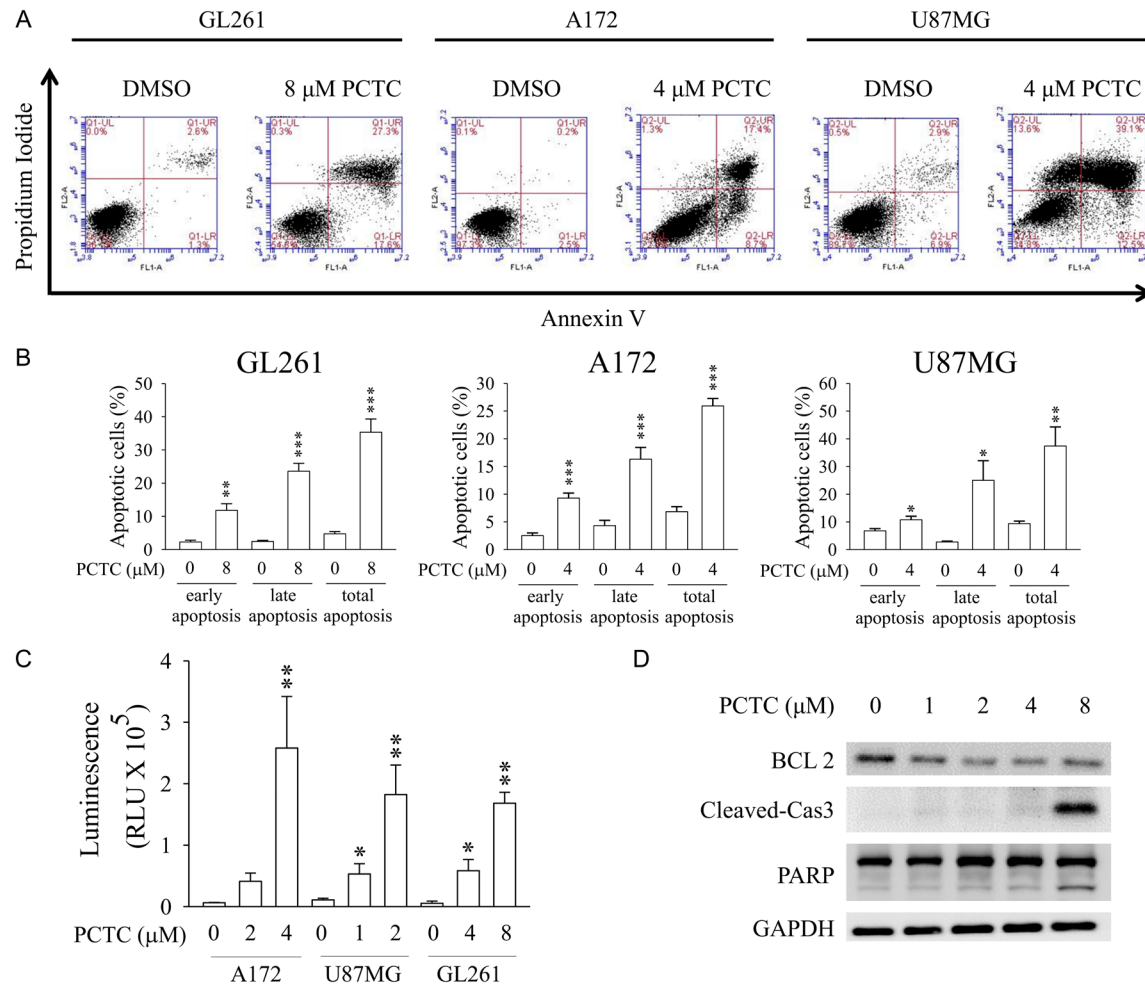


**Figure 3.** Cytotoxicity caused by apoptosis. A. Flow cytometric analysis of A172, U87MG and GL261 glioma cells treated with PCTC was performed using an Annexin V Apoptosis Detection Kit I. B. Bar graph of the percentage of apoptotic cells in flow cytometry analysis. PCTC treatment resulted in a greater increase in the apoptotic cell population in all cell types than in the control group, N=5 biological replicates. C. Luminescence measurement of Caspase-Glo® 3/7 assay showed elevation in all glioma cell lines after PCTC treatment, N=3 biological replicates. D. Western blot showed decrease in Bcl-2 and increases in cleaved-Cas 3 and PARP in GL261 cells after PCTC treatment. \*P<0.05; \*\*P<0.01; \*\*\*P<0.001, t-test.

cells and marked cell shrinkage in shape (Figure 2B and Supplementary Figure 1). Apoptotic-like morphological destruction was identified with a concentration  $\geq 4 \mu$ M. In addition, colony formation of the GL261 cells significantly decreased on day 9 after PCTC treatment (Figure 2C and 2D). This indicated that PCTC treatment had a dose-dependent cytotoxic effect on the glioma cells in vitro.

#### Induced apoptosis and reactive oxygen species production in glioma cells

To explore whether PCTC induced glioma cell death through an apoptotic mechanism, we used flow cytometry with an FITC Annexin V

Apoptosis Detection Kit I (Figure 3A). The percentages of early, late, and total apoptosis increased significantly in all three glioma cell lines after PCTC or DMSO treated for 6 hours (Figure 3B). To confirm the mechanism of PCTC-induced apoptosis, we examined the expression levels of caspase-3/7 using immunoblotting analysis. The results showed that PCTC treatment increased caspase 3/7 expressions in a dose-dependent manner in all three glioma cell lines (Figure 3C). In addition, we also examine the expressions of poly (ADP-ribose) polymerase (PARP), and Bcl-2 using Western blotting (Figure 3D). The activities of PARP were increased, however the activity of Bcl-2 was decreased. Our findings indicated

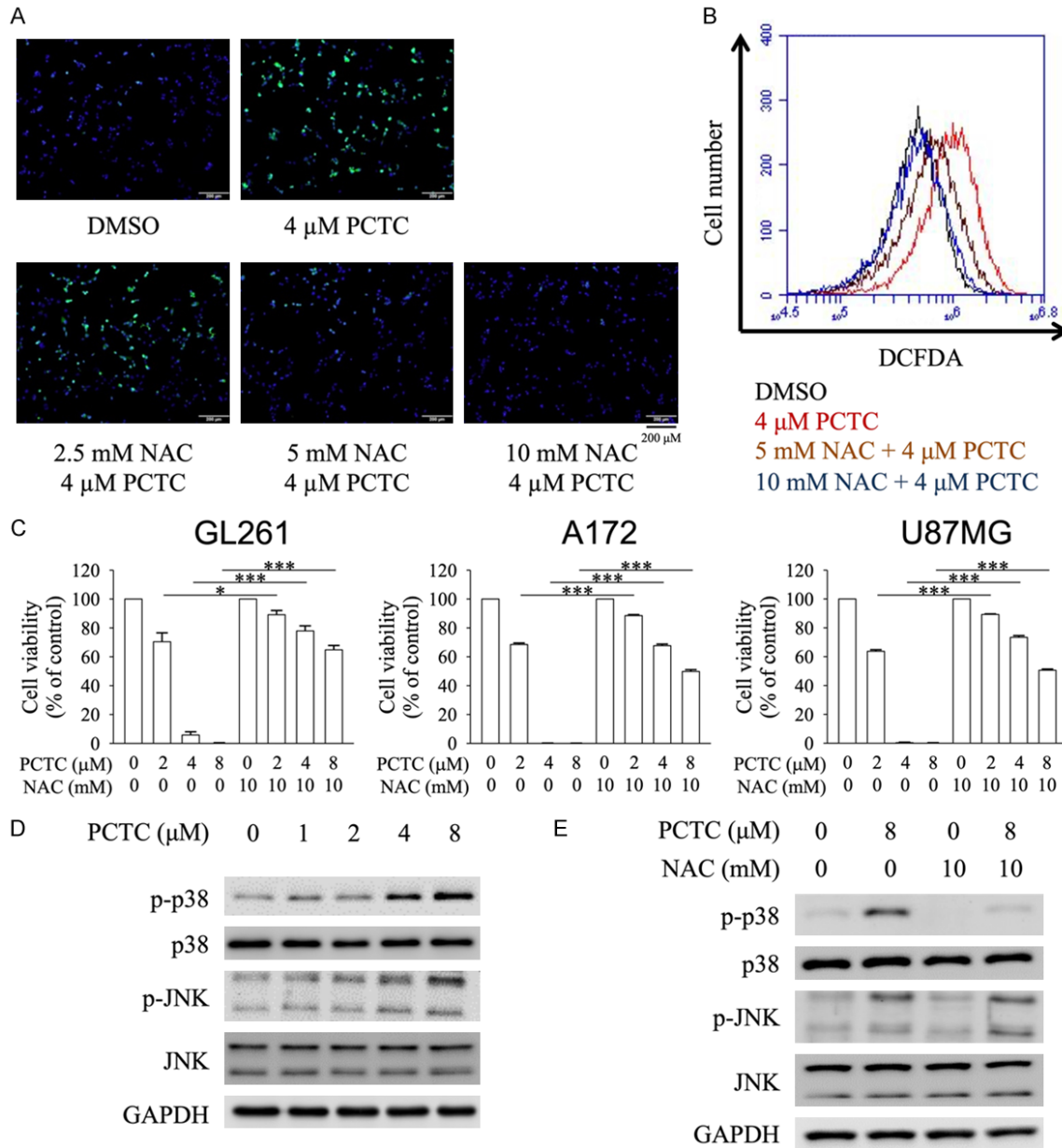


**Figure 4.** Measurement of intracellular ROS and the effects of inhibition of ROS generation on PCTC-induced cytotoxicity. A. Fluorescence microscopic analysis of iROS stained with DCFH-DA (green) within GL261 cells following treatment, which was then reversed by NAC. B. Flow cytometry analysis showed an increase in intracellular ROS in GL261 cells after PCTC treatment, which was then reversed by NAC. C. Reversed cytotoxicity by NAC within GL261, A172, U87MG cells following treatment, N=3 biological replicates. \* $P < 0.05$ ; \*\* $P < 0.01$ ; \*\*\* $P < 0.001$ , t-test. D. Western blot showed that PCTC induced ROS-dependent downstream phosphorylation of p38 and JNK. E. Western blot showed that NAC reversed the PCTC-induced phosphorylation of p38 in GL261 cells.

that PCTC induced cytotoxicity in a dose-dependent manner and provoked an apoptotic response in all three glioma cell lines.

Intracellular reactive oxygen species (iROS) were detected using DCFDA. The amount of iROS generated following treatment of these three glioma cells with PCTC 4  $\mu$ M sig-

nificantly increased. The iROS production induced by PCTC could be reversed by NAC, a free radical scavenger (Figure 4A and 4B, Supplementary Figure 2A-D), and the inhibition of cell viability by PCTC was also reversed by NAC in a dose-dependent manner (Figure 4C). Western blotting showed that p-JNK (c-Jun N-terminal kinase) and p-p38 were activated

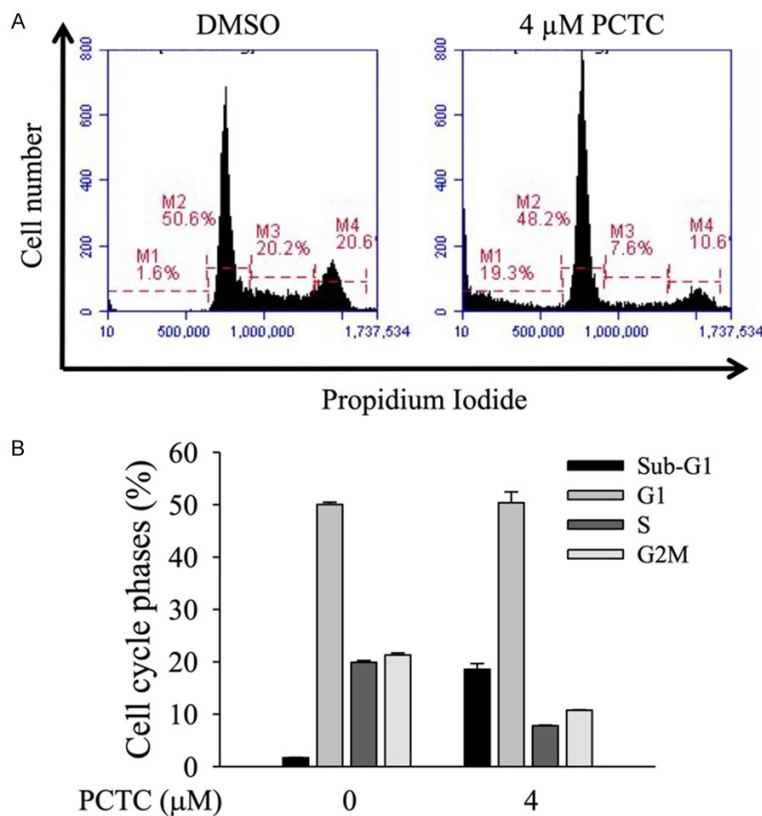


**Figure 5.** Effects of PCTC on the cell cycle distribution in GL261 cells. A. Cells were treated with DMSO and 4  $\mu$ M PCTC, and stained with PI. DNA content was analyzed for cell cycle phase distribution using flow cytometry. B. The intensities of the bands were quantified, which showed significant increases in the subG1 and decreased S phases after PCTC 4  $\mu$ M treatment. N=3 biological replicates.

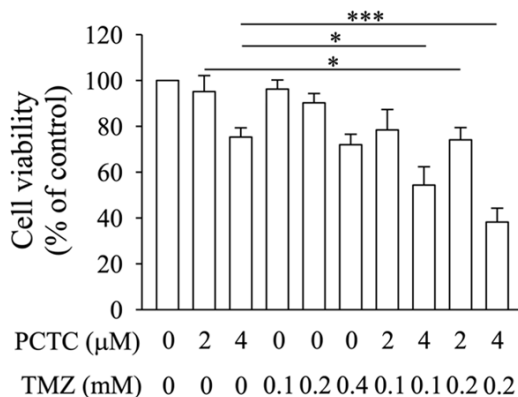


**Figure 6.** Viability of GL261 cells in vitro study. After treatment with PCTC alone, TMZ alone, and both PCTC and TMZ, significant decreased viability of GL261 in combined treatment with comparison to PCTC or TMZ alone. N=5 biological replicates. \*P<0.05, \*\*\*P<0.001, t-test.

after PCTC treatment (Figure 4D). However, p-ERK was not activated (Supplementary Figure

3). Besides, NAC could reverse the activation of p38 phosphorylation (Figure 4E). These data demonstrated that PCTC-induced apoptotic cell death may have been caused by iROS and downstream mitochondria-dependent and MAPK-mediated signaling.

#### Cell cycle arrest by PCTC

The cell cycle plays an important role in cancer cell proliferation and is also associated with apoptosis. As a result, we examined the cell cycle stage after PCTC treatment in the GL261 cells using flow cytometry (Figure 5A). The results revealed a significant increase in the subG1 phase and decreases in the S and G2 phases after 4  $\mu$ M PCTC treatment (Figure 5B). This indicated that cell cycle arrest of GL261 cells could be induced by PCTC, further leading to cytotoxicity in the GL261 cells.

#### Synergic effect of PCTC and TMZ

Temozolomide is a chemotherapy agent currently used for glioma. Several mechanisms of resistance to TMZ have been reported. We investigated whether there was a synergic therapeutic effect with a combination of TMZ and PCTC. In an in vitro cytotoxicity assay, treatment with TMZ alone (0.1 and 0.2 mM) and PCTC alone (2 and 4  $\mu$ M) showed unsatisfactory cytotoxic effects. However, treatment with both TMZ and PCTC had a strong synergic therapeutic effect. PCTC 4  $\mu$ M and TMZ 0.2 mM showed the strongest inhibitory effect on the GL261 cells (Figure 6).

#### PCTC enhanced survival in the glioma mice

Mice with GL261 cells subcutaneously implanted were untreated (control), treated with DMSO (sham), or treated with PCTC on Day 11, 14, 18 via tail vein injection (Figure 7A). Tumor growth was directly measured using a ruler. All mice treated with PCTC survived for a long period (>30 days), indicating the safety of PCTC. No

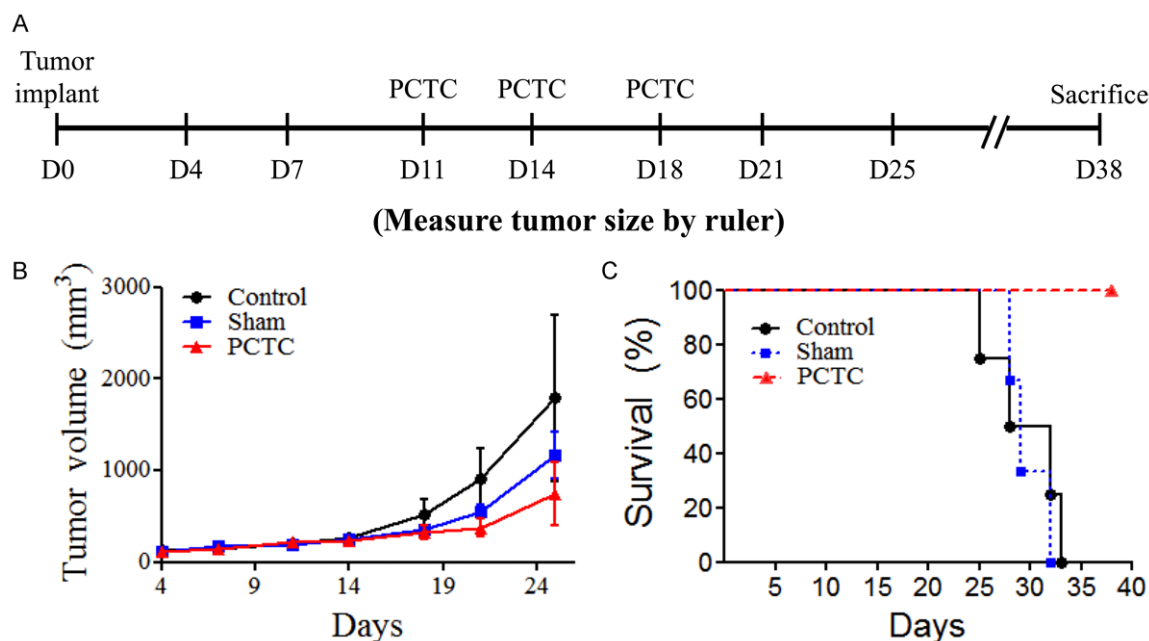


**Figure 7.** In vivo GL261 subcutaneous implantation mice model. A. After GL261 implantation in the right flank of mice (D0), PCTC was injected via the tail vein on D11, D14, and D18. B. PCTC showed a significant inhibitory effect on tumor growth compared with the control mice. C. Kaplan-Meier curves of overall survival in the tumor subcutaneous implantation mice treated with PCTC, DMSO (sham), or untreated (control). The mice treated with PCTC survived for a significantly longer time than the control and sham groups (N=3 mice in PCTC, sham, and control group).

drug-related deaths were recorded. The most significant inhibitory effect on tumor growth was found in the mice treated with PCTC (Figure 7B). In addition, the mice treated with PCTC had better survival benefits than the control and sham groups (Figure 7C). This demonstrated the safety and efficacy of PCTC in this glioma mice model.

## Discussion

### PCTC induced anticancer effects

Manzamine A, a sponge-derived  $\beta$ -carboline-fused pentacyclic alkaloid with various bioactivities, has recently been reported to have anticancer activity against pancreatic, cervical, and colorectal cancer cells [11-14]. Previous studies have reported that manzamine A-derived compounds (1-substituted carbazoyl-1, 2, 3, 4-tetrahydro- $\beta$ -carboline and carbazoyl-3, 4-dihydro- $\beta$ -carboline) demonstrated significant anticancer activities against colon adenocarcinoma DLD cells, lung large cell carcinoma NCI-H661 cells, and hepatoma HepG2/A2 cells [5, 9]. In the present study, PCTC showed dose-dependent cytotoxicity against A172, U87MG, and GL261 glioma cells. In addition, apoptotic-like morphological destruction was

seen in microscopic analysis of these three glioma cells after PCTC treatment, indicating that the cytotoxicity may have been caused by apoptosis.

Apoptosis, also known as type I programmed cell death, is a vital mechanism of anti-cancer therapeutic agents, and induction of tumor cell apoptosis is one of the best ways to treat glioma and other types of cancers [15-17]. Apoptotic death can be activated by intrinsic (mitochondrial) and extrinsic pathways. Caspase-3, a critical executioner of apoptosis, can be activated by both pathways [17, 18]. In our in vitro study, the dose of PCTC is higher for GL261 cells to achieve similar apoptotic features with A172 and U87MG cells. It probably resulted from different origin of cell line (A172 and U87MG from human, and GL261 from mouse). Nevertheless, PCTC increased the luminescence expression of caspase 3/7 in all three glioma cells, and elevated enzymatic activity of PARP but decreased the expression level of the anti-apoptotic protein Bcl-2 in GL261 cells after PCTC treatment (Figure 3C and 3D). These results indicated that apoptosis induced by PCTC was activated through a mitochondria-dependent apoptotic pathway, and resulted in further cytotoxicity of the glioma cells.



## *Role of ROS generated by PCTC in the treatment-related cytotoxicity*

The mitochondrial pathway is activated by cellular stresses, such as ROS production and mitochondrial membrane potential disruption. In addition, iROS, such as superoxide radicals, singlet oxygen, and hydrogen peroxide can induce apoptotic cell death, and also result in cytotoxicity against tumor cells. In this study, we demonstrated that iROS production was induced by PCTC, and that the inhibitory effect of cell viability by PCTC was eliminated by NAC. These findings suggest that iROS mediated cell apoptosis.

iROS have been reported to activate the MAPK signaling pathway [19]. MAPKs play crucial roles in cell survival, cell proliferation, cell cycle regulation, and apoptotic death [20, 21]. ERK, JNK, p38 kinases are three well-characterized subfamilies of MAPK [22]. Therefore, the expression levels of these three proteins were detected. Although the expression level of p-ERK was not elevated, expression levels of p-JNK and p-p38 were found to be higher after PCTC treatment. In fact, these kinases are activated in response to different apoptotic stimuli and have cross-talk between different stress and survival signaling pathways. JNK and p38 MAPK signaling pathway to mediate apoptosis and autophagy in response to these stimuli through some downstream effector [23]. Our data demonstrated PCTC induce JNK and p38 MAPK pathway activation (without ERK activation) and that this was closely linked to iROS generation. However, p38 was activated by PCTC and reversed by NAC, indicating that p-38 was regulated by iROS. In contrast, JNK was activated by PCTC but not reversed by NAC, indicating that JNK may be regulated by other mechanisms, not only by iROS. JNK and p38 both play important roles in responses to environmental stresses and inflammatory signals [24, 25]. Cross-inhibition of JNK by p38 has been reported to lead to heterogeneity in JNK activity depending on the cell type and stimulus [26]. In summary, PCTC induced iROS production and activated the MAPK pathway, both of which were related to apoptosis in glioma cells. However, further studies are needed to elucidate the detailed mechanisms by which PCTC regulates p38 and JNK.

## *Apoptosis and cell cycle arrest*

Previous studies have shown that manzamine A-derived compounds may induce cell cycle arrest at the G0/G1 phase via inhibition of cyclin-dependent kinases by p53/p21/p27. They have also been shown to trigger caspase-dependent apoptotic cell death via mitochondrial membrane potential depletion [11]. The arrest of the cell cycle is closely related with apoptosis, and cell cycle dysfunction can ultimately result in apoptotic death. Another strategy to slow tumor progression is inhibition of the deregulated cell cycle in cancer cells. Chemotherapeutic agents often cause cell cycle interruption in the G0/G1 or G2/M phase, and further enhance their anti-cancer potential [27-29]. In the present study, the obvious increase in subG1/G1 phase and significant decrease in S phase cells suggests that PCTC treatment produced a blockage effect in G1/S transition attributable to the activation of apoptosis. In general, several phase-specific regulatory proteins, commonly known as cyclins, orchestrate cell cycle progression. These proteins assemble with specific cyclin-dependent kinases (CDKs) to promote entry to the next phase. CDK4 or CDK6 activation results in G1/S phase transition [30, 31]. Ultimately, the release of retinoblastoma 1 (RB1) from transcription factors of the E2F family is induced, further leading to increased transactivation of numerous genes involved in DNA synthesis [30, 32]. Thus, PCTC may induce cell cycle arrest through the inhibition of CDK4 or CDK6. However, further investigations are needed to elucidate the detailed mechanism by which PCTC induces cell cycle arrest.

## *Combination therapy for glioma*

Temozolomide is the most commonly used chemotherapeutic agent for malignant glioma, however some patients show resistance. This has been linked to isocitrate dehydrogenase 1 (IDH1) mutations and high levels of methylation of the MGMT (O6-methylguanine DNA methyltransferase) promoter [1, 33, 34], which ultimately leads to reduced efficacy of TMZ treatment. TMZ treatment has been shown to directly target glioma cells and have toxicity at higher doses. GBM has several unique characteristics, including heterogeneity, invasion, clonal populations maintaining stem cell-like cells and recurrence, and they result in a limit-

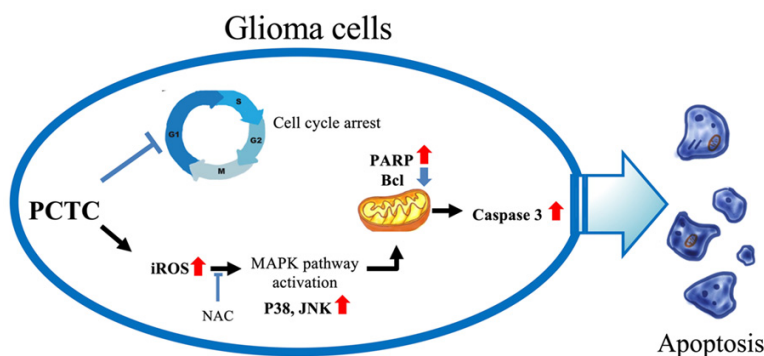


**Figure 8.** The scheme of proposed molecular mechanism induced by PCTC in glioma. In our study, PCTC activates cell cycle arrest, MAPK pathway, and apoptotic cascades, and eventually leads to apoptosis and cytotoxicity.

ed response to a variety of therapeutic approaches [4]. Combination therapy with different mechanisms to achieve better tumor control has become a trend in the treatment of GBM. In this study, we demonstrated a synergistic therapeutic effect of PCTC and TMZ in vitro against GL261 glioma cells (**Figure 6**). TMZ is an alkylating agent. Its metabolite, monomethyl triazene 5-(3-methyltriazene-1-yl)-imidazole-4-carboxamide (MTIC), can methylate DNA and cause DNA strand breaks, replicating collapse [35]. Therefore, it is known to trigger G2/M cell cycle arrest, and eventually lead to apoptosis [36]. Furthermore, PCTC-induced cell cycle blockage was shown at the G1/S transition in the present study. The synergistic effect may have been caused by blockage of different cell cycle phases by PCTC and TMZ, respectively. Therefore, the combination of PCTC and TMZ may be a clinically beneficial therapeutic strategy in the future.

#### *Antitumor effects of PCTC in the glioma subcutaneous implantation mice*

In the in vivo study, taking into consideration the potential clinical application, we treated glioma mice with PCTC systemically three times via tail vein injection. The safety of PCTC was shown as there were no drug-related deaths. We also demonstrated that PCTC significantly decreased tumor size and increased survival. These results suggest that the systemic administration of PCTC may be helpful and beneficial to achieve an anti-cancer effect. However, the intracranial microenvironment is specific and different from other organs, and the efficacy of PCTC in treating intracranial tumors is still

unclear. Further studies are needed to clarify this issue.

#### Conclusions

In this study, we found that PCTC could effectively promote cell death through apoptotic cascades and cell cycle arrest in glioma cells (**Figure 8**). Combined treatment with PCTC and TMZ had a synergistic antitumor effect on the glioma cells. Safety, efficacy, and survival benefits of PCTC treatment on glioma mice

were also demonstrated. Therefore, PCTC, a natural derivative of manzamine A, may be a clinically beneficial therapy for GBM.

#### Acknowledgements

The authors thank Aiyun Lin and Juichin Li for assistance of experiments and drawing the figures. We also acknowledged ATS Medical Editing Co. for editing this manuscript. This study is sponsored by Chang Gung Memorial Hospital (grants CMRPG2G0723), and Ministry of Science and Technology, Taiwan (110-2917-I-564-007). The sponsor had no role in the design or conduct of this research.

#### Disclosure of conflict of interest

None.

**Address correspondence to:** Tsong-Long Hwang, Chang Gung University, Taoyuan, Taiwan. E-mail: htl5523@gmail.com; Dr. Pin-Yuan Chen, Chang Gung Memorial Hospital, Keelung, Taiwan. E-mail: pinyuanc@gmail.com

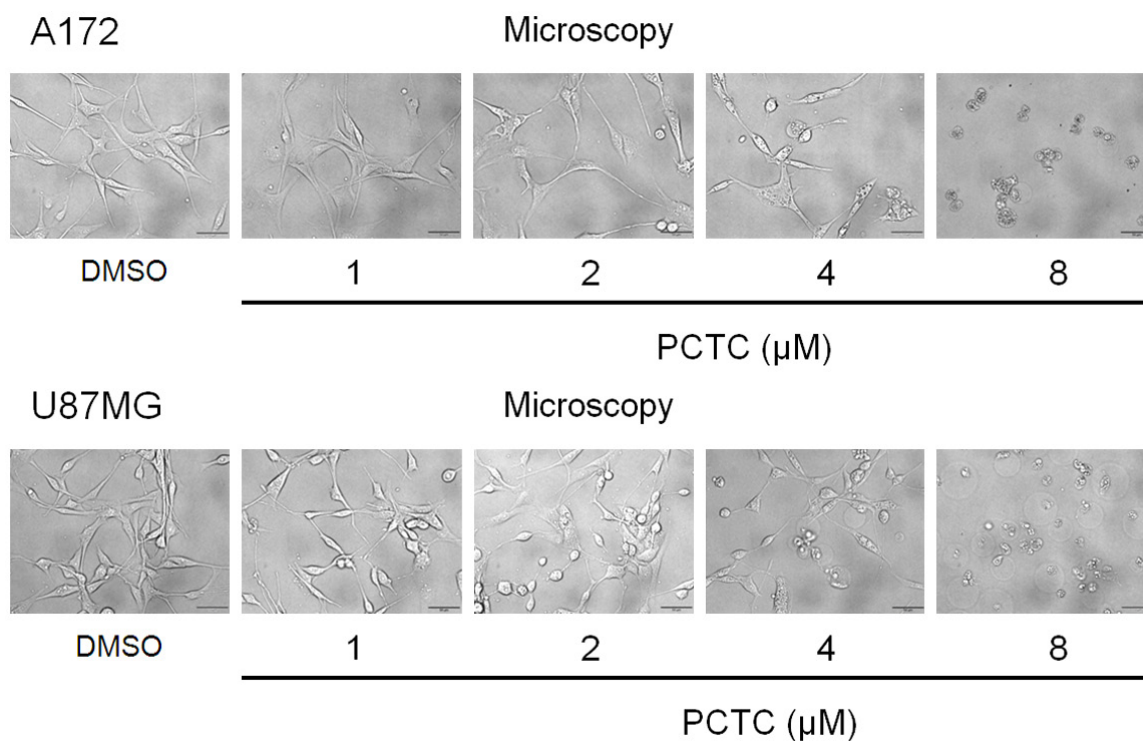
#### References

- [1] Stupp R, Mason WP, van den Bent MJ, Weller M, Fisher B, Taphoorn MJ, Belanger K, Brandes AA, Marosi C, Bogdahn U, Curschmann J, Janzer RC, Ludwin SK, Gorlia T, Allgeier A, Lacombe D, Cairncross JG, Eisenhauer E and Mirimanoff RO; European Organisation for Research and Treatment of Cancer Brain Tumor and Radiotherapy Groups; National Cancer Institute of Canada Clinical Trials Group. Radiotherapy plus concomitant and adjuvant temozolomide for glioblastoma. *N Engl J Med* 2005; 352: 987-996.

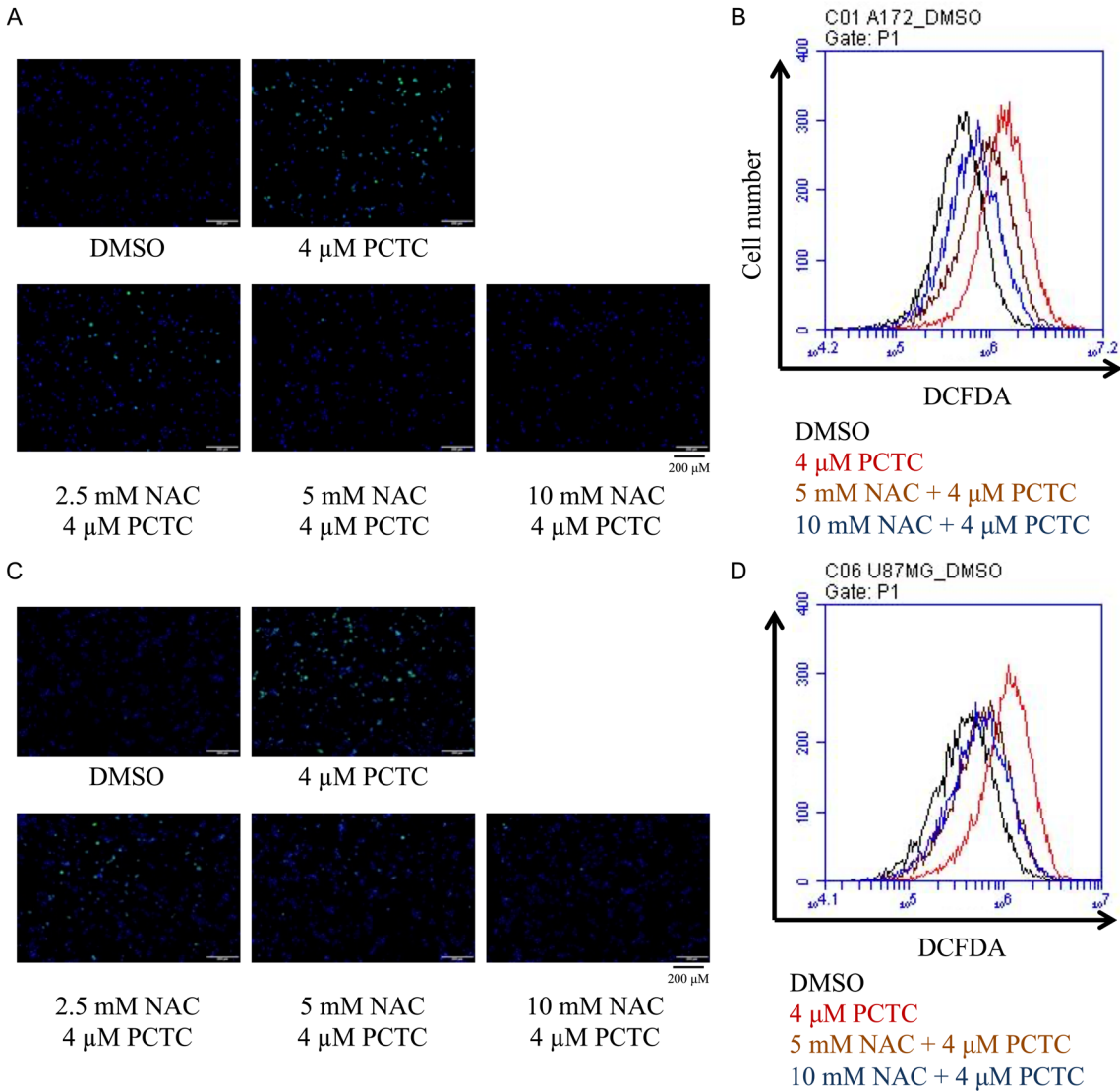
- [2] Velasquez C, Mansouri S, Mora C, Nassiri F, Suppiah S, Martino J, Zadeh G and Fernandez-Luna JL. Molecular and clinical insights into the invasive capacity of glioblastoma cells. *J Oncol* 2019; 2019: 1740763.
- [3] Ghiaseddin AP, Shin D, Melnick K and Tran DD. Tumor treating fields in the management of patients with malignant gliomas. *Curr Treat Options Oncol* 2020; 21: 76.
- [4] Cai X and Sughrue ME. Glioblastoma: new therapeutic strategies to address cellular and genomic complexity. *Oncotarget* 2018; 9: 9540-9554.
- [5] Ko PH, Shen YC, Murugan K, Huang CW, Sivakumar G, Pal P, Liao CC, Luo KS, Chuang EY, Tsai MH and Lai LC. Macrophage migration inhibitory factor acts as the potential target of a newly synthesized compound, 1-(9'-methyl-3'-carbazole)-3, 4-dihydro-beta-carboline. *Sci Rep* 2019; 9: 2147.
- [6] Shen Y, Tai H and Duh C. Bioactive constituents from *Heliclona* sp., a Formosan marine sponge. 1996.
- [7] Crews P, Cheng XC, Adamczeski M, Rodríguez J, Jaspars M, Schmitz FJ, Traeger SC and Pordesimo EO. 1, 2, 3, 4-tetrahydro-8-hydroxy-manzamines, alkaloids from two different haplosclerid sponges. *Tetrahedron* 1994; 50: 13567-13574.
- [8] Sakai R, Kohmoto S, Higa T, Jefford CW and Bernardinelli G. Manzamine B and C, two novel alkaloids from the sponge *Haliclona* sp. *Tetrahedron Lett* 1987; 28: 5493-5496.
- [9] Shen YC, Chang YT, Lin CL, Liaw CC, Kuo YH, Tu LC, Yeh SF and Chern JW. Synthesis of 1-substituted carbazolyl-1,2,3,4-tetrahydro- and carbazolyl-3,4-dihydro-beta-carboline analogs as potential antitumor agents. *Mar Drugs* 2011; 9: 256-277.
- [10] Chen PY, Wei KC and Liu HL. Neural immune modulation and immunotherapy assisted by focused ultrasound induced blood-brain barrier opening. *Hum Vaccin Immunother* 2015; 11: 2682-2687.
- [11] Lin LC, Kuo TT, Chang HY, Liu WS, Hsia SM and Huang TC. Manzamine A exerts anticancer activity against human colorectal cancer cells. *Mar Drugs* 2018; 16: 252.
- [12] Karan D, Dubey S, Pirisi L, Nagel A, Pina I, Choo YM and Hamann MT. The marine natural product manzamine A inhibits cervical cancer by targeting the SIX1 protein. *J Nat Prod* 2020; 83: 286-295.
- [13] Guzman EA, Johnson JD, Linley PA, Gunasekera SE and Wright AE. A novel activity from an old compound: manzamine A reduces the metastatic potential of AsPC-1 pancreatic cancer cells and sensitizes them to TRAIL-induced apoptosis. *Invest New Drugs* 2011; 29: 777-785.
- [14] Kallifatidis G, Hoepfner D, Jaeg T, Guzman EA and Wright AE. The marine natural product manzamine A targets vacuolar ATPases and inhibits autophagy in pancreatic cancer cells. *Mar Drugs* 2013; 11: 3500-3516.
- [15] Bogler O and Weller M. Apoptosis in gliomas, and its role in their current and future treatment. *Front Biosci* 2002; 7: e339-353.
- [16] Steinbach JP and Weller M. Apoptosis in gliomas: molecular mechanisms and therapeutic implications. *J Neurooncol* 2004; 70: 247-256.
- [17] Tsai YF, Chen YF, Hsiao CY, Huang CW, Lu CC, Tsai SC and Yang JS. Caspasedependent apoptotic death by gadolinium chloride (GdCl<sub>3</sub>) via reactive oxygen species production and MAPK signaling in rat C6 glioma cells. *Oncol Rep* 2019; 41: 1324-1332.
- [18] Pfeffer CM and Singh ATK. Apoptosis: a target for anticancer therapy. *Int J Mol Sci* 2018; 19: 448.
- [19] Zhao W, Lu M and Zhang Q. Chloride intracellular channel 1 regulates migration and invasion in gastric cancer by triggering the ROS-mediated p38 MAPK signaling pathway. *Mol Med Rep* 2016; 13: 3711.
- [20] Eblen ST. Extracellular-regulated kinases: signaling from ras to erk substrates to control biological outcomes. *Adv Cancer Res* 2018; 138: 99-142.
- [21] Faghfuri E, Nikfar S, Niaz K, Faramarzi MA and Abdollahi M. Mitogen-activated protein kinase (MEK) inhibitors to treat melanoma alone or in combination with other kinase inhibitors. *Expert Opin Drug Metab Toxicol* 2018; 14: 317-330.
- [22] Cargnello M and Roux PP. Activation and function of the MAPKs and their substrates, the MAPK-activated protein kinases. *Microbiol Mol Biol Rev* 2011; 75: 50-83.
- [23] Sui X, Kong N, Ye L, Han W, Zhou J, Zhang Q, He C and Pan H. p38 and JNK MAPK pathways control the balance of apoptosis and autophagy in response to chemotherapeutic agents. *Cancer Lett* 2014; 344: 174-179.
- [24] Cuadrado A and Nebreda AR. Mechanisms and functions of p38 MAPK signalling. *Biochem J* 2010; 429: 403-417.
- [25] Weston CR and Davis RJ. The JNK signal transduction pathway. *Curr Opin Cell Biol* 2007; 19: 142-149.
- [26] Miura H, Kondo Y, Matsuda M and Aoki K. Cell-to-cell heterogeneity in p38-mediated cross-inhibition of JNK causes stochastic cell death. *Cell Rep* 2018; 24: 2658-2668.
- [27] Pieme CA, Kumar SG, Dongmo MS, Moukette BM, Boyoum FF, Ngogang JY and Saxena AK.

- Antiproliferative activity and induction of apoptosis by *Annona muricata* (Annonaceae) extract on human cancer cells. *BMC Complement Altern Med* 2014; 14: 516.
- [28] Zorofchian Moghadamtousi S, Rouhollahi E, Karimian H, Fadaeinasab M, Firoozinia M, Ameen Abdulla M and Abdul Kadir H. The chemopotential effect of *Annona muricata* leaves against azoxymethane-induced colonic aberrant crypt foci in rats and the apoptotic effect of Acetogenin Annonamuricin E in HT-29 cells: a bioassay-guided approach. *PLoS One* 2015; 10: e0122288.
- [29] Liu N, Yang HL, Wang P, Lu YC, Yang YJ, Wang L and Lee SC. Functional proteomic analysis reveals that the ethanol extract of *Annona muricata* L. induces liver cancer cell apoptosis through endoplasmic reticulum stress pathway. *J Ethnopharmacol* 2016; 189: 210-217.
- [30] Petroni G, Formenti SC, Chen-Kiang S and Galluzzi L. Immunomodulation by anticancer cell cycle inhibitors. *Nat Rev Immunol* 2020; 20: 669-679.
- [31] Bates S, Bonetta L, MacAllan D, Parry D, Holder A, Dickson C and Peters G. CDK6 (PLSTIRE) and CDK4 (PSK-J3) are a distinct subset of the cyclin-dependent kinases that associate with cyclin D1. *Oncogene* 1994; 9: 71-79.
- [32] Kato J, Matsushime H, Hiebert SW, Ewen ME and Sherr CJ. Direct binding of cyclin D to the retinoblastoma gene product (pRb) and pRb phosphorylation by the cyclin D-dependent kinase CDK4. *Genes Dev* 1993; 7: 331-342.
- [33] Wahl M, Phillips JJ, Molinaro AM, Lin Y, Perry A, Haas-Kogan DA, Costello JF, Dayal M, Butowski N, Clarke JL, Prados M, Nelson S, Berger MS and Chang SM. Chemotherapy for adult low-grade gliomas: clinical outcomes by molecular subtype in a phase II study of adjuvant temozolomide. *Neuro Oncol* 2017; 19: 242-251.
- [34] Hegi ME, Diserens AC, Gorlia T, Hamou MF, de Tribolet N, Weller M, Kros JM, Hainfellner JA, Mason W, Mariani L, Bromberg JE, Hau P, Mirimanoff RO, Cairncross JG, Janzer RC and Stupp R. MGMT gene silencing and benefit from temozolomide in glioblastoma. *N Engl J Med* 2005; 352: 997-1003.
- [35] Zhang J, Stevens MF and Bradshaw TD. Temozolomide: mechanisms of action, repair and resistance. *Curr Mol Pharmacol* 2012; 5: 102-114.
- [36] Alonso MM, Gomez-Manzano C, Bekele BN, Yung WK and Fueyo J. Adenovirus-based strategies overcome temozolomide resistance by silencing the O6-methylguanine-DNA methyltransferase promoter. *Cancer Res* 2007; 67: 11499-11504.

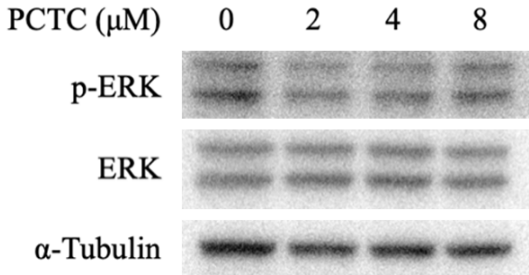




**Supplementary Figure 1.** Microscopic analysis showed apoptotic-like morphological destruction after different doses of PCTC treatment for 24 hours in the human glioma cells (A172 and U87MG).



**Supplementary Figure 2.** Fluorescence microscopic analysis of iROS (stained with DCFH-DA (green)) and flow cytometry following PCTC treatment within A172 (A and B) and U87MG (C and D) glioma cells, which was then reversed by NAC respectively. N=3 biological replicates. T-test, \*\*\*P<0.001.



**Supplementary Figure 3.** Western blot showed no phosphorylation of ERK in GL261 cells following PCTC treatment.